Polymer Journal (2016) 48, 635–643

www.nature.com/pj

ORIGINAL ARTICLE

Effect of varying the composition and nanostructure of organic carbonate-containing lyotropic liquid crystal polymer electrolytes on their ionic conductivity

Robert L Kerr[1,4], Julian P Edwards[1,5], Simon C Jones[2,6], Brian J Elliott[3] and Douglas L Gin[1]

Nanostructured composite electrolyte films consisting of a cross-linked lyotropic liquid crystal (LLC) monomer, an organic carbonate liquid electrolyte (propylene carbonate, dimethylcarbonate, diethylcarbonate) and a Li salt ($LiClO_4$, $LiBF_4$, $LiPF_6$) were systematically prepared and characterized at two electrolyte concentrations (0.245 and 1.0 M) and four liquid loading levels (5, 15, 30, 50 wt %). The LLC morphology of the films was investigated using polarized light microscopy and powder X-ray diffraction; their ionic conductivity was investigated using AC impedance measurements. Higher liquid electrolyte loadings and Li salt concentrations generally increased ionic conductivity, regardless of the liquid electrolyte or salt used. Some mixed-phase LLC morphologies displayed good ionic conductivity; however, as initially prepared, these formulations were at the limit of liquid uptake. In contrast, composites with a type II bicontinuous cubic (Q_{II}) LLC phase containing ordered, three-dimensional interconnected nanopores exhibited good conductivity using much less liquid electrolyte and a lower Li salt concentration, indicating that this structure is more amenable to ion transport than less ordered/uniform morphologies. When wetted with electrolyte solution and integrated into Li/fluorinated carbon coin cells, the Q_{II} films were sufficiently strong to act as an ion-conductive separator and displayed stable open-circuit potentials. Many of the mixed-phase films gave shorted cells.
Polymer Journal (2016) **48,** 635–643; doi:10.1038/pj.2015.119; published online 27 January 2016

INTRODUCTION

Lithium-metal batteries represent a form of high energy density storage in current and future electrical device applications. Li provides the highest cell potential (−3.04 V vs H^+/H_2) and the lowest density of any metal.[1–4] Currently, mass-produced Li-metal cells are found in the primary (that is, non-rechargeable) cell configuration only; secondary (that is, rechargeable) Li-metal cells have yet to compete with the Li-ion cells that dominate the battery market.[4–10] The use of Li metal as a rechargeable battery anode is potentially very promising if significant issues can be overcome, in particular metal dendrite formation between the electrodes during recharging (leading to a short circuit).[4,7–10]

The separator membrane is a key component of Li batteries, acting as a dedicated pathway allowing Li ions to pass through from the anode to the cathode during discharge while physically separating the two electrodes in the cell to prevent short-circuiting. The separator membrane must allow facile ion transport, be thermally stable, show good mechanical properties, be lightweight and permit handling under normal manufacturing conditions (see ref. 11 for a recent overview of nanostructured LC- and polymer-based ion-conductive materials).[11] Inert macro- and microporous materials (for example, porous polyethylene and polypropylene) are commonly used as separator membranes in Li-ion batteries. Ion transfer between the cathode and anode is accomplished via an added liquid electrolyte that wets the separator. This electrolyte is typically an organic liquid with dissolved Li salt, although these electrolytes have challenges such as high loadings required of Li salt, flammability and toxicity. Concerns have also been raised regarding the thermomechanical stability of the separator membrane during recharging and periods of high rate discharge, since higher temperatures can lead to softening of these membranes, resulting in an internal short. Nevertheless, inert polymers combined with non-aqueous liquid electrolytes, and various gel polymer variants, have typically been the media of choice for lithium battery separator membrane technologies.[1–4,10,12–14]

Ion-conductive polymer electrolytes represent a 'single-component' alternative to this mixture of inert polymer and liquid electrolyte.[11] Amorphous polymers such as poly(ethylene oxide) and other weak Lewis basic polymers such as poly(propylene oxide) can be utilized in several ways. These polymers can be doped with Li salts,[8,15–17] made into melt-blended composites that are solvent-free, and utilized in

[1]Department of Chemistry and Biochemistry, University of Colorado, Boulder, CO, USA; [2]Contour Energy Systems, Inc., Azusa, CA, USA and [3]TDA Research, Inc., Wheat Ridge, CO, USA
[4]Current address: ITT Cannon, LLC, MTC Labs, 666 E. Dyer Road, Santa Ana, CA 92705, USA
[5]Current address: Division of Chemistry and Chemical Engineering, MC 164-30 CH, California Institute of Technology, Pasadena, CA 91125, USA
[6]Current address: Electrochemical Technologies Group, NASA-JPL, 4800 Oak Grove Drive, Pasadena, CA 91109, USA
Correspondence: Professor DL Gin, Department of Chemistry and Biochemistry, University of Colorado, UCB 424, Boulder, CO 80309, USA.
E-mail: gin@spot.colorado.edu
Received 3 October 2015; revised 17 November 2015; accepted 21 November 2015; published online 27 January 2016

gelled systems containing utilizing Li salt–liquid electrolyte solutions. Although these electrolytes have lower conductivities ($\leqslant 10^{-4}$ S cm^{-1}) compared with common liquid electrolytes ($\geqslant 10^{-3}$ S cm^{-1}), they have the advantage of being 'dry', and are easier to handle in manufacturing.[8,15–17] However, blended poly(ethylene oxide)-based polymer electrolytes have poor low-temperature conductivity owing to loss of segmental motion of the polymer chains. Cooling the polymer below its glass transition temperature (T_g) negatively impacts conductivity due to the decrease in motion. Addition of additives such as liquid electrolytes, Li salts, plasticizers or inorganic fillers have improved Li-ion conductivity through lowering of the T_g and increasing void volume in the polymer.[1–3,12,18]

Ordered solid electrolytes that contain permanent, continuous pathways allow efficient ion transport and therefore can display higher conductivities.[17,18] One recent approach to making polymeric versions of this type of ordered electrolyte material has focused on nanophase-separated block copolymers containing an ion-conductive block (see ref. 19 for a recent review of phase-separated block copolymer-based electrolyte materials and their application to lithium batteries).[19] Another approach to making polymer electrolytes with ordered, ion-conductive, nanoscale domains has focused on using liquid crystal (LC) components, which display a degree of average molecular order similar to crystals but retain some fluidity like an isotropic liquid.[20] These LC electrolyte systems can be thermotropic (that is, neat materials that change their degree of order as a function of temperature only), or they can be lyotropic (that is, amphiphilic materials that can change their degree of order as a function of the amount of an added fluid and temperature).[20] Their ordered, fluid-like environments could be important for better ion mobility in conductive applications.

Research utilizing temperature-dependent, solvent-free (that is, thermotropic) LC ion-conducting systems has covered a wide variety of approaches, including the use of molecular (that is, non-polymerized)[21–30] and linear polymer-connected LC ion-conducting units.[31–37] Unfortunately, the typical room-temperature ionic conductivity values of prior thermotropic LC materials were generally found to be around $\sim 10^{-6}$ S cm^{-1}, and the LC order important for conductivity in these materials can vary significantly with temperature as a result of phase changes.[21–37] Only two thermotropic LC electrolyte systems have been reported that exhibit higher conductivity values (that is, $\geqslant 10^{-3}$ S cm^{-1}) at room temperature,[28,37] one of which utilized varying amounts of hydration to facilitate ion mobility.[28] However, LC materials with temperature-stable ionic conductivity behavior can be made by heavily cross-linking the thermotropic LC electrolyte moieties into ordered polymer networks,[38–41] but there is some sacrifice in ionic conductivity with the associated loss of LC mobility upon polymer network formation.[39] It has also been found that the dimensionality of the order in LC-based solid electrolytes is also important for ionic conductivity. Solvent-free bicontinuous cubic thermotropic LC phases with three-dimensional interconnected ionic domains were found to afford higher conductivities than LC phases with one-dimensional or two-dimensional ordered ionic regions.[26] Cross-linked bicontinuous cubic thermotropic LC materials have been found to show this same nanostructure-ionic conductivity trend.[40,41] Very recent work has also shown that Li-salt-doped, non-polymerizable, thermotropic LC materials with a smectic (that is, layered) nanostructure can be effectively used as the electrolyte in Li test cells.[42] To our knowledge, this work represents the first time that thermotropic LC-based electrolytes have been demonstrated to successfully function in a Li battery application.

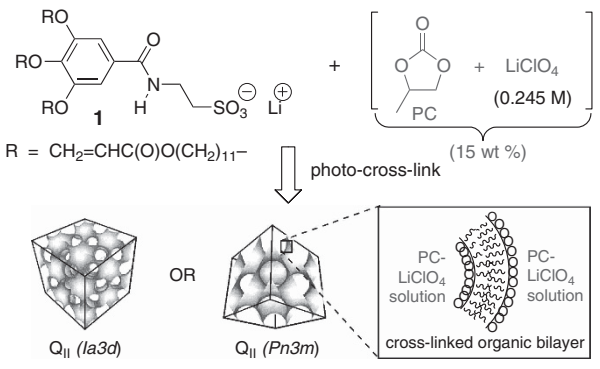

Figure 1 Structure of the nanostructured Li-ion-conducting solid–liquid composite electrolyte based on the cross-linking of a Q_{II} phase formed by LLC monomer **1** around a PC–$LiClO_4$ solution. Reproduced with permission from ref. 48. Copyright 2009 American Chemical Society. LLC, lyotropic liquid crystal; PC, propylene carbonate. A full color version of this figure is available at *Polymer Journal* online.

In 2009, we reported a new type of organic electrolyte material that combines desirable features of LC-based solid electrolytes (average molecular order), polymers (processibility and mechanical stability) and liquid electrolytes (high intrinsic ion diffusion) in a single material. This new electrolyte material is a nanostructured, polymer–liquid composite based on the self-organization and ordered microphase-separation of an ionic LLC monomer (**1**) around a conventional Li salt-doped liquid electrolyte solution ($LiClO_4$ in PC; Figure 1).[48] After *in situ* photo-radical cross-linking of monomer **1** in this environment, a solid–liquid composite is formed that contains a type II (that is, inverse) bicontinuous cubic (Q_{II}) structure with three-dimensional interconnected nanochannels containing a Li-salt-doped liquid electrolyte solution.[48] The resulting polymer–liquid nanocomposite is a very flexible, optically transparent film material that does not leach out the liquid electrolyte solution. Films of this Q_{II}-phase composite material containing 15 wt % (0.245 M $LiClO_4$ in PC) were found to consistently afford ionic conductivity values of 10^{-4} to 10^{-3} S cm^{-1} at room temperature.[48] These conductivity values were also retained down to sub-ambient temperatures as low as -65 °C.[48] Consequently, this new LLC polymer-based composite electrolyte overcomes several shortcomings of conventional polymer (for example, poly(ethylene oxide)) and gelled polymer lithium battery electrolyte approaches, such as poor low-temperature performance due to a low T_g,[1–4,12] the high liquid electrolyte loading levels (40–70 wt %) needed for good room-temperature conductivity,[5,8,9,49,50] and the potential for (flammable and toxic) liquid electrolyte leaching.[5,8,9,49,50]

In the present work, we describe systematic variation of the liquid carbonate electrolyte and Li salt dopant in our cross-linked LLC composite electrolyte material to access different LLC phases. After the compositions were completed and cross-linked for stability of handling, their morphologies were investigated by polarized light microscopy (PLM) and powder X-ray diffraction (PXRD) to determine the type of LLC order present. AC impedance measurements were then utilized to identify the compositions with high room-temperature conductivities. Specifically, the organic liquid electrolytes tested were PC, dimethylcarbonate (DMC) and diethylcarbonate (DEC); and the Li salt dopants tested were $LiClO_4$, $LiBF_4$ and $LiPF_6$ (all commonly used in lithium battery construction). The most promising film compositions were then integrated in CR2025-type coin cells containing a Li metal anode and a fluorinated carbon (CF_x) cathode (that is, Li/CF_x cells) to determine their mechanical robustness/suitability in battery fabrication. Only a very small number of publications has reported testing of newly synthesized nanostructured organic electrolyte materials in actual batteries.[42,51]

From these collective studies, we found that in general, the use of higher salt dopant content in the liquid electrolyte solutions afforded higher bulk ion conductivities in the resulting composites, as would be expected. However, higher loading levels of the same doped liquid electrolyte solution usually did not always result in samples with higher bulk ionic conductivities. Ionic conductivity and AC impedance performance varied considerably with the type of liquid electrolyte and Li salt dopant used, and also with the type of LLC phase formed. Consequently, there did not appear to be any easily identified correlations between sample chemical composition, sample morphology and AC impedance figures of merit. Interestingly, we found that the compositions that exhibited some of the highest ionic conductivity values in this system did not always require a specific, well-defined LLC-phase structure (that is, a Q_{II} phase) to be present. In fact, compositions that afforded less-defined, mixed LLC-phase morphologies often exhibited room-temperature ionic conductivities comparable to or higher than that of the original Q_{II}-phase material. However, these materials (as initially prepared) were at the limit of liquid loading (~50 wt %) and displayed some phase separation and surface wetting by excluded liquid electrolyte solution. When wetted with electrolyte solution and integrated into test coin cells, the majority of these less uniformly ordered, mixed LLC-phase films resulted in shorted cells. In contrast, it was found that films with a well-defined Q-phase morphology were not only able to maintain good ionic conductivity with lower liquid electrolyte loading but also afforded films of sufficient mechanical stability when wetted with electrolyte solution to allow fabrication of coin cells with stable open-circuit potentials.

MATERIALS AND METHODS

Materials and general procedures

Battery-grade or better PC, DMC, DEC, $LiPF_6$, $LiBF_4$ and $LiClO_4$ were all purchased from the Sigma-Aldrich Chemical Company (St Louis, MO, USA) and used as received, unless otherwise stated. All other reagents and solvents used for the preparation of the monomer **1** and the polymerization of its composite samples were purchased from Fluka (Buchs, Switzerland), Sigma-Aldrich or Mallinkrodt (St Louis, MO, USA), and purified and used as described previously.[48] Monomer **1** was synthesized and purified according to the procedures detailed in our prior publication.[48] Chemical structure and purity characterization data were consistent with published values.[48] Fluorinated carbon (CF_x, $x=0.9$, graphitic precursor) cathodes were provided by Contour Energy Systems (Azusa, CA, USA) used as received (CF_x:PVDF:Super-P carbon = 85:5:10 (w/w/w)). CR2025 battery cans and internals (seals, springs, spacers and so on) were purchased from Hohsen (Osaka, Japan). The Li metal foil was purchased from FMC Lithium (Charlotte, NC, USA). TDA Research provided access to the following equipment for lithium battery preparation and testing: a Vacuum Atmospheres Company Light VAC HE303 drybox for sample preparation/battery assembly, a Hohsen manually operated coin-cell battery press with CR2025 dies, and a MACCOR Model 4300 Desktop Automated Test System for battery voltage testing. Battery materials were handled and assembled in a dry argon (Ar) atmosphere unless otherwise noted, using dry solvents and samples unless otherwise noted.

Instrumentation

PXRD spectra were obtained with an Inel CPS 120 diffraction system (Artenay, France) using Cu K_α radiation. PXRD measurements on samples were all performed at ambient temperature ((21 ± 2) °C). The LLC mixtures were mixed using an IEC (Needham Heights, MA, USA) Centra-CL2 centrifuge. The LLC film samples were radically photo-cross-linked between fused silica (quartz) slides at ambient temperature and under an inert Ar environment in a Scienceware acrylic portable glovebox. A Spectroline XX-15A UVA (365 nm) lamp (Westbury, NY, USA) or an EXTECH (Nashua, NH, USA) UV-LED (365 nm) with a DC power supply was used as the photopolymerization light source. UV light fluxes at the sample surface were measured using a Spectroline DRC-100X digital radiometer equipped with a DIX-365 UV-A sensor. Electrochemical impedance spectroscopy were conducted using an Agilent (Santa Clara, CA, USA) HP 4284A (20 Hz to 1 MHz) or an HP 4194A (100 Hz to 110 MHz) AC impedance analyzer connected to a stainless-steel and PTFE test cell that was made in-house at the University of Colorado Department of Chemical and Biological Engineering Machine Shop.[48]

Preparation and assembly

General procedure for preparing LLC phases. The appropriate amount of pure monomer **1** was first weighed into a tared, clean, dry glass microtube (10 mm I.D. and 30 mm length) made by the Glass Shop in the Department of Chemistry and Biochemistry in a Scienceware glovebox under Ar purge. The appropriate weight of anhydrous electrolyte-salt solution was then added to the microtube by micropipette. The desired amount (1 wt %) of radical photo-initiator, 2-hydroxy-2-methylpropiophenone, was then added by micropipette. The microtube was immediately sealed to prevent evaporation of the electrolyte solution, and also to prevent absorption of water. The sealed microtube was then placed in an aluminum block heater set at (55.5 ± 0.5) °C for 6 min to thermally equilibrate. After 6 min, the microtube and contents were centrifuged at 3800 r.p.m. for 25 min. The contents of the microtube were then mixed by hand using a small spatula inside the Ar-filled portable glovebox with the sealing film left in place for 3 min. The centrifuge–hand mix process was then repeated a total of four times, placed between glass slides, and gently compressed but not sheared. The resulting material was then viewed under the PLM for the presence or absence of birefringence. (The absence of birefringence can be suggestive of an isotropic phase, as well as a Q phase.) This process (with subsequent PLM texture analysis) was repeated with precise amounts of electrolyte–salt solution added to the original monomer mixture to produce a given composition.

This material was then transferred to a preheated ((55.0 ± 0.5) °C) quartz plate. A spacer of the desired thickness (for example, 80 μm) was placed in on the same face as the individual electrolyte monomer **1** mixture. Another preheated quartz plate (same dimensions and temperature as the first) was then placed directly on top of the first plate, thereby sandwiching the LLC monomer phase between the plates. The sandwiched sample was then placed on an aluminum block heater to maintain the temperature at (55.5 ± 0.5) °C for 2 min, removed from the heater, and then clamped with three to four large alligator clips, depending on the sample size. Gentle downward hand pressure was exerted on the quartz plates until the LLC monomer gel stopped flowing due to the film thickness spacers. The sandwiched sample was then allowed to cool (~1 h) undisturbed to room temperature ((21 ± 2) °C) and then placed under the 365 nm UV lamp for cross-linking for 65 min at a UV light flux of 660 μW cm^{-2} at the sample surface. The film was then photo-cross-linked, viewed again under PLM to determine that the phase was identical to that of the unpolymerized sample, and then analyzed by PXRD to quantitatively identify the specific LLC phase formed. See Supplementary Figure S1 for pictures of this film formation and cross-linking process.

Electrochemical impedance spectroscopy/AC impedance testing of cross-linked 1/liquid electrolyte solution composites. Electrochemical impedance spectroscopy/AC impedance measurements to determine ionic conductivity were performed as previously described in our prior publication.[48] Complete details on the measurement method and calculations used are also provided in the Supplementary Information.

Assembly and open-circuit voltage testing of prepared lithium-metal batteries. All components of the battery were introduced into an Ar-filled drybox. Cathodes were supplied in sealed, moisture-proof containers. Li metal foil (~0.025 inches thick), and the LLC membranes were cut with a 16-mm-diameter punch die by hand by applying light, continuous, downward pressure while gently rotating the die ±30° on a PTFE or HDPE slab. A CR2025 cell can, the anode, the cathode, the LLC separator membrane, the seal, the spacer and the spring were assembled with the electrolyte solutions in preparation of assembly (see Supplementary Figure S4). Once all the materials were positioned in an assembly-line fashion in the drybox (see Supplementary Figure S5), the Li metal foil was placed into the anode side of the can (smaller diameter can, see Supplementary Figure S5, #1 and 2). Three microliters of doped electrolyte solution was then applied to the surface of the Li metal foil to adequate wet it. Concurrently, the cathode material and cross-linked membrane of **1** were soaked separately in an excess of doped electrolyte solution until they could not absorb additional electrolyte. This was followed by bubbling out of the entrapped gas from the porous cathode material and complete surface wetting of the cross-linked composite. When the bubbling ceased, the cathode was removed from the doped electrolyte solution and placed on a non-reactive HDPE substrate until ready for use. Next (see Supplementary Figure S5, #3), the wetted cross-linked composite membrane was lifted from its wetting solution, and the excess was allowed to drain off the surface for about 30 s. It was then placed onto the Li-metal foil surface. A unidirectional seal (see Supplementary Figure S5, #4) was then placed onto the ring of the can containing the Li metal and the cross-linked composite membrane. The cathode was then placed onto the membrane (see Supplementary Figure S5, #5), followed by a stainless-steel spacer onto the cathode (see Supplementary Figure S5, #6). The remaining empty CR2025 cell half was then placed on top of the sandwiched assembly, slid to the edge and inverted, taking care not to handle the activated cell with any metal objects that would cause the cell to short immediately. It was then moved to a Hohsen battery-crimping machine, with a CR2025 die set, for the final hermetic/mechanical seal.

Once the battery was crimped, it was removed and placed into a zip-top bag to ensure it would not have contact with any metal, which could produce a cell short. Once the cells were completely assembled, they were removed and tested (within 1 h of assembly) with the MACCOR 4300 Desktop Automated Test System or a low-impedance voltage meter that were set up outside the drybox. Three separate instantaneous readings were taken, and the average open-circuit voltage values with standard deviation error bars were reported.

RESULTS AND DISCUSSION

LLC monomer **1** was prepared and purified as previously described in our first publication on this system.[48] The composites/LLC mixtures of **1** containing the selected liquid electrolytes (PC, DMC and DEC), the Li salt dopants ($LiClO_4$, $LiBF_4$ and $LiPF_6$), and a small amount (1 wt %) of a radical photo-initiator were made according to the procedures described in our prior publication.[48] The only variation was the type and amount of doped liquid electrolytes that were added to the monomer for investigation (see the Materials and methods section for details). The mixtures were then radically photo-cross-linked by UV light (365 or 375 nm) to generate free-standing film samples with stability for handling. The cross-linked samples were then examined by PLM to determine whether the material showed LLC behavior with a particular doped liquid electrolyte solution. The cross-linked composites were then analyzed by PXRD to help quantitatively identify the LLC phase or phases present.[48]

The three organic carbonate-based liquid electrolytes (PC, DMC and DEC) chosen for this initial composition variation study were selected because they are commonly used in the construction of commercial Li batteries,[1–3,52] and our prior work showed that **1** is able to form LLC phases with PC instead of water.[48] Although it is common in the Li battery industry to use binary and even ternary mixtures of DMC, DEC, PC and other solvents as liquid electrolyte solutions, we have chosen to investigate only single-component liquid electrolyte systems for simplicity and also for ease of handling and testing. The initial choice of Li salts ($LiPF_6$, $LiBF_4$ and $LiClO_4$) was also based on commercial availability and prior precedence in the literature.[1–3]

To facilitate testing but still obtain a representative sampling of the large number of composition permutations possible, doped electrolyte solutions were made and initially tested at 0.245 and 1.0 M using the three selected Li salt dopants. The 0.245 M concentration value is one that is already known to work in PC solutions of **1** from prior work,[48] and the 1.0 M value is typically the concentration of doped liquid electrolyte solutions used in commercial or test batteries.[1–3,52] With different combinations of the three liquid electrolytes and three Li salts made into separate 0.245 and 1.0 M test solutions, it was decided to explore their LLC-phase formation with monomer **1** at total liquid electrolyte loading levels of 5, 15, 30 and 50 wt % of the total composite mixture. These values were selected to give a good and rapid initial scan of the phase behavior of monomer **1** in these different liquid electrolyte/Li salt solutions. Mixtures containing >50 wt % electrolyte solution were explored, but they all showed distinct signs of macrophase separation (that is, visible liquid electrolyte exclusion). With these samples, composition of matter could not be guaranteed, and therefore samples with >50 wt % total liquid loading were excluded from further testing. This observation also put a practical limit on the maximum amount of liquid electrolyte solution incorporated into our sample composition studies. It is also important to stress that the type of LLC phase (or lack thereof) present in the samples was not a parameter for choosing which samples to investigate for bulk ionic conductivity determination via AC impedance analysis.

It should also be noted that one detrimental issue that arose with handling of the $LiPF_6$ salt dopant was its propensity to readily react with moisture and create HF (a well-known byproduct of the decomposition of the PF_6^- anion). The $LiPF_6$ solutions turned out to be difficult to handle and were found to decompose in a relatively short time period (that is, 48 h) at ambient temperature after mixing with the monomer (although we did not observe this with $LiBF_4$). Consequently, we chose to limit the preparation and testing of the number of samples after the first round of phase formation was completed instead of making and testing the full range of compositions as in the case of the other two Li salts.

In total, 56 different compositions (out of the 72 possible permutations) were prepared based on monomer **1**, the three different liquid electrolytes, and the three Li salts, using two different solution concentrations (0.245 and 1.0 M) and four different total liquid electrolyte solution loading levels in the mixture. After UV-initiated radical cross-linking to preserve the morphologies of these mixtures for ease of handling and further analysis, the 56 different samples in film form were then characterized by PLM and visual inspection to determine if a LLC phase formed. The identities of any observed LLC phases were then determined by both PLM and PXRD analyses, as described previously in our prior publication.[48] All film samples were then analyzed by AC impedance measurements[53–56] to determine their ionic conductivity using the same method described in our prior publication.[48] Finally, six of the most promising new formulations, along with the initial Q_{II}-phase material (that is, containing 15 wt % (0.245 M $LiClO_4$ in PC)) were integrated as the separator material in

Table 1 Summary data for the eight most notable compositions of 1, liquid electrolyte solution and Li salt dopant that showed either a well-defined LLC phase or one of the highest ionic conductivities

Film #	*Doped liquid electrolyte solution*	*Solution loading (wt %)*	*LLC phase*	*PLM optical texture*	*PXRD peaks (Å)*	*Extrapolated solution resistance (Ω)*	*Ionic conductivity (S cm^{-1})*	*Li/CF$_x$ cell open-circuit potential (V)*
F2	0.245 M $LiClO_4$ in PC	15	Q_{II}	Black	***35.6, 31.1, 29.4, 27.2, 26.9, 24.1, 20.2***	7	1.0E−03	Stable, (3.5±0.2)
F4	0.245 M $LiClO_4$ in PC	50	Mixed[a]	Biref.	***34.6***	115	1.1E−04	Stable, (3.29±0.06)
F8	1.0 M $LiClO_4$ in PC	50	Mixed[a]	Biref.	***35.6, 29.2, 27.1, 26.1(br)***	27	5.4E−04	Stable, (3.4±0.3)
F24	1.0 M $LiClO_4$ in DMC	50	Mixed[a]	Biref	*34.3, 33.2, 28.3,* ***26.6***	1	1.8E−03	Not tested
F51	1.0 M $LiBF_4$ in DEC	30	Mixed	Biref.	33.2, ***26.8,25.6, 24.5,*** *14.9(br)*	3.8	4.6E−03	Unstable, (0.007±0.002)
F53	1.0 M $LiPF_6$ in DEC	5	Mixed	Biref.	**34.8, 29.4, 27.0, 25.4, 24.4, 20.2(br)**	9	8.1E−04	Unstable, 0.053
F55	1.0 M $LiPF_6$ in DEC	30	Mixed	Biref.	***35.0, 29.4, 27.0, 25.6, 24.4, 20.2(br)***	6.4	9.7E−04	Unstable, 0.012
F56	1.0 M $LiPF_6$ in DEC	50	Mixed[a]	Biref.	*38.2,* ***34.8, 28.9, 26.8, 20.2(br)***	2.6	3.1E−03	Unstable, 0.812

Abbreviations: LLC, lyotropic liquid crystal; PLM, polarized light microscopy; PXRD, powder X-ray diffraction.
[a]Appearance of visible macrophase separation and liquid exclusion from the sample; mixed, mixed LLC phase; iso, isotropic phase (no order); biref., birefringent.
PXRD peaks: italic print indicates peaks with relative maxima; bold print indicates peaks that can be indexed to a Q_{II} phase; (br) indicates broad peak.

CR2025-format Li/CF$_x$ coin cells and their open-circuit voltage measured as a preliminary guide to the mechanical stability of these films in a battery assembly.

The full characterization data for the 56 different samples of **1**, liquid electrolyte and Li salt dopant prepared in this study are listed in their entirety in three tables in the Supplementary Information, based on the type of liquid electrolyte used (see the Supplementary Tables S1–S3). Because of the large amount of data generated for the LLC phase and AC impedance characterization of the 56 different compositions, only the most overt observed trends and relationships between composition, sample morphology and AC impedance results are summarized and discussed, as a matter of practicality.

On the basis of the general down-selection criteria described above, Table 1 below summarizes the most notable compositions of **1**, liquid electrolyte and Li salt dopant that showed high ionic conductivity, along with data on the original Q_{II}-phase sample containing 15 wt % (0.245 M $LiClO_4$ in PC) from our initial paper on this system[48] for comparison purposes. The data in Table 1 show the polymerized film sample number (as per the labeling system in the Supplementary Information); the chemical composition of each sample; the type of LLC phase/morphology present as determined by PLM and PXRD analysis; the ionic conductivity properties of each film as determined by AC impedance studies and preliminary mechanical stability of the film as a separator in a Li/CF$_x$ coin cell as determined from the cell open-circuit potential.

With respect to LLC-phase identification, Q LLC phases can be easily identified by the presence of a black (that is, pseudo-isotropic/non-birefringent due to the cubic symmetry) PLM optical texture and PXRD *d*-spacings (that is, diffraction peaks) that proceed as $1/\sqrt{6}:1/\sqrt{8}:1/\sqrt{9}:1/\sqrt{10}$ and so on (see ref. 59 for a recent review of cross-linked Q-phase LLC materials and their applications).[48,57–59] Other common LLC phases such as lamellar (that is, stacked two-dimensional bilayers) and hexagonal (that is, close-packed cylindrical columns) exhibit birefringent (that is, bright) PLM optical textures because they are anisotropic assemblies in the bulk polydomain state. The lamellar and hexagonal phases can be quantitatively identified by having PXRD *d*-spacings that proceed as 1:1/2:1/3:1/4 and so on, and $1:1/\sqrt{3}:1/\sqrt{4}:1/\sqrt{7}$ and so on, respectively, which are a direct consequence of their unit cell geometries (see ref. 60 for a general review of LLC phases).[60–62] Type I (that is, normal) and type II (inverse) versions of these LLC phases can be inferred from whether the phase in question appears on the solvent-rich or solvent-lean side of the lamellar phase in an ideal LLC-phase-diagram progression.[60–62] Amorphous (that is, non-ordered/non-LLC) samples have a black PLM texture and no observed PXRD peaks owing to their isotropic/non-periodic nature.[60–62] When samples exhibited a birefringent optical texture as well as PXRD peaks (clearly indicating the presence of a LLC phase), but the PXRD peaks cannot be indexed to a single LLC phase or easily de-convoluted, these samples were categorized as 'mixed' LLC phases for the purposes of this study.

Figure 2 shows the PXRD profiles and PLM optical textures of as-prepared, cross-linked films of the eight compositions listed in Table 1. Also of note is that the as-prepared samples that showed visible evidence of macrophase separation or liquid exclusion were identified as such in Table 1, as well as in the full data tables for all 56 samples in the Supplementary Information. The presence of bulk liquid electrolyte solution on the surface of samples can lead to higher than expected ionic conductivity/very low resistance because ions can easily move around the sample via the very mobile bulk liquid on the surfaces. However, this is not an accurate representation of the actual ionic conductivity through the film and can lead to short circuiting of the test cell or device. AC impedance measurements were made as described in the prior literature.[48] Extrapolation to the x-intercept point of the plot of real (R) vs imaginary (X) resistance provided the solution resistance for the respective samples.[48,53–56]

In examining the data for all the 56 sample compositions (see the Supplementary Information) to arrive at the films presented in Table 1, we found that there were no obvious correlations between sample chemical composition, morphology and ionic conductivity. The only general trend appeared to be that the use of higher Li salt dopant concentrations in the electrolyte solutions generally afforded higher bulk ion conductivities in the resulting composites, as would be expected. Surprisingly, increasing the wt % loading of a particular Li salt-doped electrolyte solution usually did not always result in higher ionic conductivities in the samples. However, the bulk ionic conductivity varied considerably with the type of liquid electrolyte and Li salt dopant used, and also with the LLC phase formed. Interestingly, it was found that the compositions that exhibited the highest observed

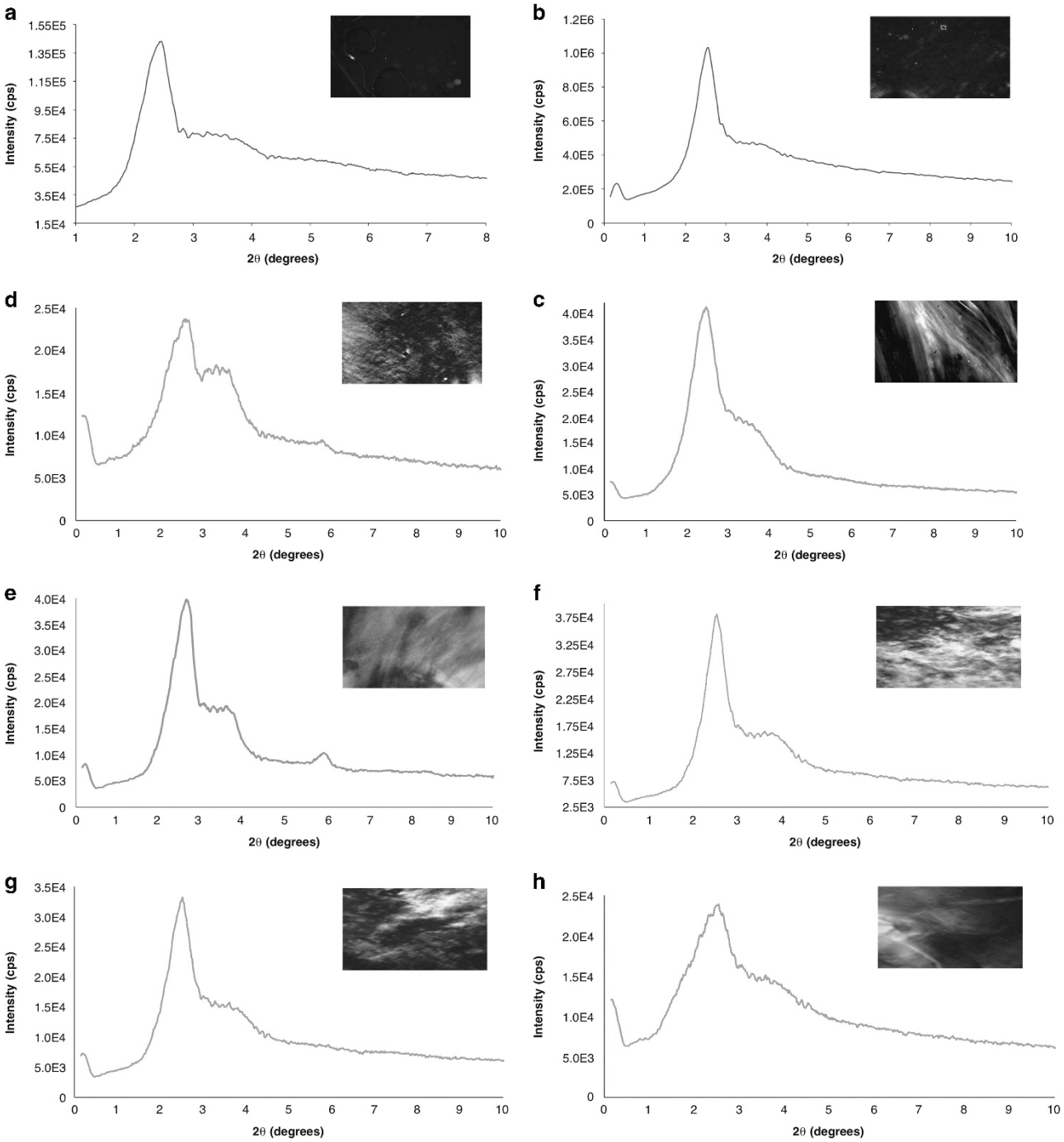

Figure 2 PXRD profiles with inset PLM optical textures (×10 magnification) for the cross-linked film samples listed in Table 1: (**a**) **F2**, (**b**) **F4**, (**c**) **F8**, (**d**) **F24**, (**e**) **F51**, (**f**) **F53**, (**g**) **F55** and (**h**) **F56**. PLM, polarized light microscopy; PXRD, powder X-ray diffraction. A full color version of this figure is available at *Polymer Journal* online.

ionic conductivity values did not always require a specific, well-defined LLC-phase structure (i.e., a Q_{II} phase) to be present. In fact, compositions that afforded less-defined, mixed LLC-phase morphologies often exhibited good room-temperature ionic conductivity values, sometimes more than twice that of the original Q_{II}-phase material containing 15 wt % (0.245 M) $LiClO_4$ in PC (film **F2**; 1.0×10^{-3} S cm^{-1}). The samples that showed this high ionic conductivity ($\geqslant \sim 2.0 \times 10^{-3}$ S cm^{-1}) varied considerably with the type and amount of liquid electrolyte and Li salt dopant present and with film morphology. (See the yellow-highlighted films in the Supplementary Information tables: **F11–F13** made with doped PC (Supplementary Table S1); **F17**, **F21–F23**, **F25**, **F32–F36** made with doped DMC (Supplementary Table S2); **F43**, **F46**, **F49–F52**, **F56** made with doped DEC (Supplementary Table S3).). No readily discernible chemical composition-property or structure-property trends can be identified from these data, except that regardless of sample morphology, compositions made with $LiBF_4$- and $LiPF_6$-doped DMC and DEC solutions were more likely to afford higher conductivity samples than

those made with doped PC solutions. An interesting side-note with respect to the morphologies of the majority of the films that exhibited mixed LLC phases of the 56 total samples is that their PXRD profiles showed at least two *d*-spacings that index well to a Q phase (that is, 1/$\sqrt{6}$:1/$\sqrt{8}$…; see the bold-faced PXRD peaks listed in the Supplementary Information Tables S1–S3).[57–59] This result implies that the Q_{II} phase is one of the LLC phases present in these mixed-phase samples (to some degree), even though it was often difficult to pinpoint the black regions in their overall birefringent PLM optical textures. This result also reinforces the observation made in our prior paper that monomer **1** has a very strong tendency to form the Q_{II} phase (and no other LLC phases) under a variety of conditions.[48]

Although analysis of the data for the samples did not reveal any clear trends between chemical composition, morphology/LLC phase and ionic conductivity in this new materials system, application of these films as separator structures in simple coin cells did reveal certain differences between the materials. CR2025 coin cells were constructed using Li metal foil as the anode, a fluorinated carbon-based (CF_x where $x = 0.9$) cathode active material; and films **F2**, **F4**, **F8**, **F51**, **F53**, **F55** and **F56** were wetted with liquid electrolyte and used as the separator membrane between the two electrolyte-wetted electrodes. The open-circuit voltage values of the resulting cells were then measured after crimping. In all the test cells, the membrane film thickness was maintained at (70 ± 20) μm.

As shown in Table 1, the sample compositions based on monomer **1** that had the highest measured bulk ionic conductivity values (**F51** and **F56**) gave cells with an unstable open-circuit potential significantly lower than that expected (>3 V),[63] indicating that the cells had internal shorts of varying degrees of severity. Similar behavior was exhibited by cells made from films **F53**, **F55** and **F56.** These films were all mixed LLC-phase samples in terms of their morphology. The electrically shorted behavior exhibited by their respective Li/CF_x cells suggests that these mixed LLC phases do not feature sufficient mechanical strength for successful integration into coin cells. Conversely, stable, high open-circuit voltages were exhibited by cells containing a mixed LLC phase made with high liquid electrolyte loading (50 wt %), which is at the threshold of liquid exclusion/phase-separation in the as-prepared films (**F4** and **F8**). This result may be a result of these particular high liquid electrolyte-templated samples having a more macroporous, open structure (due to liquid exclusion/macrophase-separation during initial cross-linking) that is able to hold on to more liquid electrolyte solution internally and at the surface when wetted for cell integration. This would enable better ion transport through and interfacial contact between the electrodes and the separator film (that is, the separator is behaving more as a phase-separated, high-electrolyte-loaded and 'surface-pooled' heterogeneous film rather than a 'drier' (that is, lower electrolyte-containing), homogeneous composite film). However, this feature is not really practical for integration into a working cell, and may lead to the same problems related to liquid electrolyte exclusion/phase-separation discussed in the Introduction. Finally, cells featuring the cross-linked Q_{II}-phase composite of **1** containing 15 wt % (0.245 M $LiClO_4$ in PC, **F2**) were found to display a high, stable open-circuit potential despite having less liquid electrolyte during film formation. Although **F2** has only 15 wt % loading of a lower Li salt concentration electrolyte solution (generally lower than the other samples tested), its distinguishing feature is the presence of a well-defined Q_{II}-phase nanostructure (no liquid exclusion upon cross-linking) with three-dimensional-interconnected liquid electrolyte nanopores. Hence, this structure features both mobile ions and sufficient mechanical strength for cell integration.

This general observation reinforces what our group and other research groups have previously observed with bicontinuous cubic lyotropic and thermotropic LC materials having superior transport properties over materials with lower dimensionality.[11,26–29,40,41,48,59] The interconnectivity and ordered nanoscale transport channels inherent in the Q LLC phases affords a pore system that is not only difficult to completely block but also alleviates the need for bulk sample alignment to obtain high throughput for transport applications. These features make polymers based on Q phases much more amenable to transport and membrane applications compared with other LC phases and morphologies.[59] These transport effects for Q-type LLC materials have been observed previously in membrane selectivity, flux and AC-impedance-based ionic conductivity measurements.[11,48,59] However, we believe that this study represents the first time that this effect has been observed in a Li battery configuration with a lyotropic LC material serving as an ion-conducting separator membrane.

Summary

In summary, a systematic series of 56 cross-linked composite electrolyte films consisting of LLC monomer **1**, an organic carbonate-based liquid electrolyte (PC, DMC or DEC), and a small Li salt dopant ($LiClO_4$, $LiBF_4$ or $LiPF_6$) were prepared and tested at two different electrolyte solution concentrations (0.245 and 1.0 M) and at four liquid loading levels (5, 15, 30 and 50 wt % total). Their phase morphology was investigated using PLM and PXRD. Their bulk ionic conductivity properties at room temperature were investigated using AC impedance measurements. Seven of the most promising films were then incorporated into CR2025-format battery assemblies. It was found that a well-defined Q-phase morphology in these systems afforded films of sufficient mechanical stability to allow fabrication of Li/CF_x coin cells with stable open-circuit potentials. In general, higher electrolyte content and higher salt concentrations in the composite samples investigated were found to increase the ionic conductivity regardless of the type of liquid or Li salt dopant. A number of mixed-phase LLC morphologies (without a well-defined LLC structure) displayed high bulk ionic conductivity similar to, or greater than, the Q_{II} phase. The majority of these mixed-phase LLC films were not strong enough to survive the coin-cell fabrication procedure intact, resulting in shorted cells. In certain cases, Li/CF_x coin cells with stable open-circuit potential could be made from mixed LLC-phase morphology films. However, we believe that these materials should not be considered to be useful 'dry' composites. The morphologies of these mixed-phase films are more disordered and likely macroporous because they were formed and cross-linked at compositions at the limit of liquid uptake (~50 wt %). That is, these films displayed some phase separation and surface wetting by excluded liquid electrolyte solution during initial preparation, and this structural heterogeneity is trapped in the resulting materials after cross-linking. Ultimately, this investigation suggests that a cross-linked Q_{II}-phase can act as a suitably conductive separator membrane for Li batteries at lower electrolyte loadings (~33% of that in the mixed-phase samples) because its ordered, three-dimensional-interconnected liquid nanopore structure is more amenable to transport of ions than more disordered or discontinuous phase-separated morphologies.

Although these Q_{II}-phase composite electrolytes show promise in these initial tests, cell discharge and cycling studies need to be done on these new materials before their viability for battery use can be determined. It is also possible to make thinner films of these and related Q-phase LLC polymer composites in free-standing and supported film configurations[59] as a means of potentially improving

cell performance. These are directions for additional future work in this area.

CONFLICT OF INTEREST

The authors declare no conflict of interest.

ACKNOWLEDGEMENTS

This work was funded by the U.S. Department of Energy via an STTR Grant to TDA Research with a subcontract to CU Boulder (DE-FG02-04ER84093) and the NSF Liquid Crystal Materials Research Center at CU Boulder (DMR-0820579).

1 Besenhard, J. O. *Handbook of Battery Materials* 1st edn (Wiley-VCH, Weinheim, Germany, 1999).
2 Schlesinger, H. *The Battery* (HarperCollins, New York, NY, USA, 2010).
3 Vincent, C. A. & Scrosati, B. *Modern Batteries. An Introduction to Electrochemical Power Sources* 2nd edn (Arnold, London, UK, 1997).
4 Xu, K. Nonaqueous liquid electrolytes for lithium-based rechargeable batteries. *Chem. Rev.* **104**, 4303–4417 (2004).
5 Croce, F., D'Epifanio, E. A., Hassoun, J., Reale, P. & Scrosati, B. Advanced electrolyte and electrode materials for lithium polymer batteries. *J. Power Sources* **119–121**, 399–402 (2003).
6 Saunier, J. A., Alloin, F., Sanchez, J. Y. & Caillon, G. Thin and flexible lithium-ion batteries: investigation of polymer electrolytes. *J. Power Sources* **119**, 454–459 (2003), and references within.
7 Scrosati, B., Croce, F. & Panero, S. Progress in lithium polymer battery R&D. *J. Power Sources* **100**, 93–100 (2001).
8 Song, J. Y., Wang, Y. Y. & Wan, C. C. Review of gel-type polymer electrolytes for lithium-ion batteries. *J. Power Sources* **77**, 183–197 (1999), and references therein.
9 Vincent, C. A. Lithium batteries: a 50-year perspective, 1959–2009. *Solid State Ionics* **134**, 159–167 (2000).
10 Zaghib, K. & Kinoshita., K. Advanced materials for negative electrodes in Li-polymer batteries. *J. Power Sources* **125**, 214–220 (2004).
11 Kato, T. From nanostructured liquid crystals to polymer-based electrolytes. *Angew. Chem. Int. Ed.* **49**, 7847–7848 (2010).
12 Gray, F. M. *Solid Polymer Electrolytes* 1st edn (VCH Publishers, New York, NY, USA, 1991).
13 Lewandowski, A., Olejniczak, A., Galinski, M. & Stepniak, I. Performance of carbon–carbon supercapacitors based on organic, aqueous and ionic liquid electrolytes. *J. Power Sources* **195**, 5814–5819 (2010), and references within.
14 Lewandowski, A. & Swiderska–Mocek, A. Performance of carbon–carbon supercapacitors based on organic, aqueous and ionic liquid electrolytes. *J. Power Sources* **194**, 601–609 (2009).
15 Megahed, S. & Ebner, W. J. Lithium-ion battery for electronic applications. *J. Power Sources* **54**, 155–162 (1995).
16 Scrosati, B. Recent advances in lithium ion battery materials. *Electrochim. Acta* **45**, 2461–2466 (2000), and references therein.
17 Wright, P. V. Developments in polymer electrolytes for lithium batteries. *Mater. Res. Soc. Bull.* **27**, 597–602 (2002).
18 Funahashi, M., Shimura, H., Yoshio, M. & Kato, T. Functional liquid-crystalline polymers for ionic and electronic conduction. *Struct. Bond.* **128**, 151–179 (2008).
19 Young, W. -S., Kuan, W. -F. & Epps, T. H. III Block copolymer electrolytes for rechargeable lithium batteries. *J. Polym. Sci. B Polym. Phys.* **52**, 1–16 (2014).
20 Collins, P. J. *Liquid Crystals: Nature's Delicate State of Matter* (Princeton Univ. Press, Princeton, 1990).
21 Kimura, K., Hirao, M. & Yokoyama, M. Synthesis of a crowned azobenzene liquid crystal and its application to thermoresponsive ion-conducting films. *J. Mater. Chem.* **1**, 293–294 (1991).
22 Shimura, H., Yoshio, M., Hamasaki, A., Mukai, T., Ohno, H. & Kato, T. Electric-field-responsive lithium-ion conductors of propylene carbonate-based columnar liquid crystals. *Adv. Mater.* **21**, 1591–1594 (2009).
23 Ohtake, T., Takamitsu, Y., Ito–Akita, K., Janie, K., Yoshizawa, M., Mukai, T., Ohno, H. & Kato, T. Liquid-crystalline ion-conductive materials: self-organization behavior and ion-transporting properties of mesogenic dimers containing oxyethylene moieties complexed with metal salts. *Macromolecules* **33**, 8109–8111 (2000).
24 Hoshino, K., Kanie, K., Ohtake, T., Mukai, T., Yoshizawa, M., Ujiie, S., Ohno, H. & Kato, T. Ion-conductive liquid crystals: formation of stable smectic semi-bilayers by the introduction of perfluoroalkyl moieties. *Macromol. Chem. Phys.* **203**, 1547–1555 (2002).
25 Yoshio, M., Mukai, T., Ohno, H. & Kato, T. One-dimensional ion transport in self-organized columnar ionic liquids. *J. Am. Chem. Soc.* **126**, 994–995 (2004).
26 Ichikawa, T., Yoshio, M., Hamasaki, A., Mukai, T., Ohno, H. & Kato, T. Self-organization of room-temperature ionic liquids exhibiting liquid-crystalline bicontinuous cubic phases: formation of nano-ion channel networks. *J. Am. Chem. Soc.* **129**, 10662–10663 (2007).
27 Ichikawa, T., Yoshio, M., Hamasaki, A., Taguchi, S., Liu, F., Zeng, X. -B., Ungar, G., Ohno, H. & Kato, T. Induction of thermotropic bicontinuous cubic phases in liquid-crystalline ammonium and phosphonium salts. *J. Am. Chem. Soc.* **134**, 2634–2643 (2012).
28 Ichikawa, T., Kato, T. & Ohno, H. 3D continuous water nanosheet as a gyroid minimal surface formed by bicontinuous cubic liquid-crystalline zwitterions. *J. Am. Chem. Soc.* **134**, 11354–11357 (2012).
29 Soberats, B., Yoshio, M., Ichikawa, T., Taguchi, S., Ohno, H. & Kato, T. 3D anhydrous proton-transporting nanochannels formed by self-assembly of liquid crystals composed of a sulfobetaine and a sulfonic acid. *J. Am. Chem. Soc.* **135**, 15286–15289 (2013).
30 Soberats, B., Uchida, E., Yoshio, M., Kagimoto, J., Ohno, H. & Kato, T. Macroscopic photocontrol of ion-transporting pathways of a nanostructured imidazolium-based photoresponsive liquid crystal. *J. Am. Chem. Soc.* **136**, 9552–9555 (2014).
31 Tokuhisa, H., Yokoyama, K. & Kimura, K. Photoinduced switching of ionic conductivity by metal ion complexes of vinyl copolymers carrying crowned azobenzene and biphenyl moieties at the side chain. *J. Mater. Chem.* **8**, 889–891 (1988).
32 Dias, F. B., Batty, S. V., Gupta, A., Ungar, G., Voss, J. P. & Wright, P. V. Ionic conduction of lithium, sodium and magnesium salts within organised smectic liquid crystal polymer electrolytes. *Electrochim. Acta* **43**, 1217–1224 (1998).
33 Yue, Z., McEwen, I. J. & Cowie, J. M. G. Ion conducting behaviour and morphology of solid polymer electrolytes based on a regioselectively substituted cellulose ether with PEO side chains. *J. Mater. Chem.* **12**, 2281–2285 (2002).
34 Hoshino, K., Yoshio, M., Mukai, T., Kishimoto, K., Ohno, H. & Kato, T. Nanostructured ion-conductive films: layered assembly of a side-chain liquid-crystalline polymer with an imidazolium ionic moiety. *J. Polym. Sci. A Polym. Chem* **41**, 3486–3492 (2003).
35 Kishimoto, K., Yoshio, M., Mukai, T., Yoshizawa, M., Ohno, H. & Kato, T. Nanostructured anisotropic ion-conductive films. *J. Am. Chem. Soc.* **125**, 3196–3197 (2003).
36 Judestein, P. & Roussel, F. Ionic conductivity of lithium salt/oligo(ethylene oxide)-based liquid-crystal mixtures: The effect of molecular architecture on the conduction process. *Adv. Mater.* **17**, 723–727 (2005).
37 Kishimoto, K., Suzawa, T., Yotoka, T., Mukai, T., Ohno, H. & Kato, T. Nano-segregated polymeric film exhibiting high ionic conductivities. *J. Am. Chem. Soc.* **127**, 15618–15623 (2005).
38 Beginn, U., Zipp, G., Mourran, A., Walther, P. & Möller, M. Membranes containing oriented supramolecular transport channels. *Adv. Mater.* **12**, 513–516 (2000).
39 Yoshio, M., Kagata, T., Hoshino, K., Mukai, T., Ohno, H. & Kato, T. One-dimensional ion-conductive polymer films: Alignment and fixation of ionic channels formed by self-organization of polymerizable columnar liquid crystals. *J. Am. Chem. Soc.* **128**, 5570–5577 (2006).
40 Ichikawa, T., Yoshio, M., Hamasaki, A., Kagimoto, J., Ohno, H. & Kato, T. 3D interconnected ionic nano-channels formed in polymer films: Self-organization and polymerization of thermotropic bicontinuous cubic liquid crystals. *J. Am. Chem. Soc.* **133**, 2163–2169 (2011).
41 Zhang, H., Li, L., Möller, M., Zhu, X., Rueda, J. J. H., Rosenthal, M. & Ivanov, D. A. From channel-forming ionic liquid crystals exhibiting humidity-induced phase transitions to nanostructured ion-conducting polymer membranes. *Adv. Mater.* **25**, 3543–3548 (2013).
42 Sakuda, J., Hosono, E., Yoshio, M., Ichikawa, T., Matsumoto, T., Ohno, H., Zhou, H. & Kato, T. Liquid-crystalline electrolytes for lithium-ion batteries: ordered assemblies of a mesogen-containing carbonate and a lithium salt. *Adv. Funct. Mater.* **25**, 1206–1212 (2015).
43 Yoshio, M., Mukai, T., Kanie, K., Yoshizawa, M., Ohno, H. & Kato, T. Liquid-crystalline assemblies containing ionic liquids: an approach to anisotropic ionic materials. *Chem. Lett.* **32**, 320–321 (2002).
44 Shimura, H., Yoshio, M., Hoshino, K., Mukai, T., Ohno, H. & Kato, T. Noncovalent approach to one-dimensional ion conductors: enhancement of ionic conductivities in nanostructured columnar liquid crystals. *J. Am. Chem. Soc.* **130**, 1759–1765 (2008).
45 Ichikawa, T., Yoshio, M., Taguchi, S., Kagimoto, J., Ohno, H. & Kato, T. Co-organisation of ionic liquids with amphiphilic diethanolamines: construction of 3D continuous ionic nanochannels through the induction of liquid–crystalline bicontinuous cubic phases. *Chem. Sci.* **3**, 2001–2008 (2012).
46 Sakuda, J., Yoshio, M., Ichikawa, T., Ohno, H. & Kato, T. 2D assemblies of ionic liquid crystals based on imidazolium moieties: formation of ion-conductive layers. *New J. Chem.* **39**, 4471–4477 (2015).
47 Soberats, B., Yoshio, M., Ichikawa, T., Ohno, H. & Kato, T. Zwitterionic liquid crystals as 1D and 3D lithium ion transport media. *J. Mater. Chem. A* **3**, 11232–11238 (2015).
48 Kerr, R. L., Miller, S. A., Shoemaker, R. K., Elliot, B. J. & Gin, D. L. New type of Li ion conductor with 3D interconnected nanopores via polymerization of a liquid organic electrolyte-filled lyotropic liquid-crystal assembly. *J. Am. Chem. Soc.* **131**, 15972–15973 (2009).
49 Morford, R. V. A phosphate additive for poly(ethylene oxide)-based gel polymer electrolytes. *Solid State Ionics* **177**, 721–726 (2006).
50 Murata, K., Izuchi, S. & Yoshihisa, Y. An overview of the research and development of solid polymer electrolyte batteries. *Electrochim. Acta* **45**, 1501–1508 (2000).
51 Bouchet, R., Maria, S., Meziane, R., Aboulaich, A., Lienafa, L., Bonnet, J. -P., Phan, T. N. T., Bertin, D., Gigmes, D., Devaux, D., Denoyel, R. & Armand, M. Single-ion BAB triblock copolymers as highly efficient electrolytes for lithium-metal batteries. *Nat. Mater.* **12**, 452–457 (2013).

52 Masias, A. J., Neil, M. & Bohn, T. P. *Advanced Battery Technology, 2010* (SAE International, Warrendale, PA, USA, 2010).
53 Gamry Instruments. Application Notes (2015). http://www.gamry.com/APP_Notes/EIS_Primer/EIS_Primer.htm. Accessed October 1, 2015.
54 Bard, A. J. & Faulkner, L. R. *Electrochemical Methods; Fundamentals and Applications* (Wiley Interscience, New York, NY, USA, 2000).
55 Barsoukov, E. & MacDonald, J. R. *Impedance Spectroscopy; Theory, Experiment, and Applications* 2nd edn (Wiley Interscience, New York, NY, USA, 2005).
56 *Electrochemical Impedance, Analysis and Interpretation* (eds Scully, J. R., Silverman, D. C. & Kendig, M. W.) (ASTM, Philadelphia, PA, USA, 1993).
57 Mariana, P., Luzzati, V. & Delacroix, H. Cubic phases of lipid-containing systems: structure analysis and biological implications. *J. Mol. Biol.* **204**, 165–189 (1988).
58 Pindzola, B. A., Jin, J. & Gin, D. L. Cross-linked normal hexagonal and bicontinuous cubic assemblies via polymerizable gemini amphiphiles. *J. Am. Chem. Soc.* **125**, 2940–2949 (2003), and references therein.
59 Wiesenauer, B. R. & Gin, D. L. Nanoporous polymer materials based on self-organized, bicontinuous cubic lyotropic liquid crystal assemblies and their applications. *Polym. J.* **44**, 461–468 (2012).
60 Tiddy, G. J. T. Surfactant-water liquid crystal phases. *Phys. Rep.* **57**, 1–46 (1980).
61 Seddon, J. M. Structure of the inverted hexagonal (H_{II}) phase, and non-lamellar phase transitions of lipids. *Biochim. Biophys. Acta* **1031**, 1–69 (1990).
62 Hyde, S. T. in *Handbook of Applied Surface and Colloid Chemistry* (ed. Holmberg, K.) Ch. 16 (John Wiley & Sons, New York, NY, USA, 2001).
63 Linden, D. & Reddy, T. B. in *Handbook of Batteries* 3rd edn (eds Linden, D. & Reddy, T. B.) Ch.14 (McGraw-Hill, New York, NY, USA, 2002).

Supplementary Information accompanies the paper on Polymer Journal website (http://www.nature.com/pj)